Influence of forest and shrub canopies on precipitation partitioning and isotopic signatures

Journal:	Hydrological Processes
Manuscript ID	HYP-17-0447.R1
Wiley - Manuscript type:	Research Article
Date Submitted by the Author:	n/a

Complete List of Authors:	Soulsby, Chris; University of Aberdeen, School of Geosciences Braun, Hannah; University of Aberdeen, Northern Rivers Institute; University of Freiburg, Chair of Hydrology Sprenger, Matthias; University of Aberdeen, Northern Rivers Institute, School of Geosciences Weiler, Markus; University of Freiburg, Institute of Hydrology; Tetzlaff, Doerthe; University of Aberdeen, Northern Rivers Institute, School of Geosciences

Keywords:	Forest hydrology, interception, throughfall, isotopes, Canopy, Boreal forest

Influence of forest and shrub canopies on precipitation partitioning and isotopic signatures

C. Soulsby[1], H. Braun[1,2], M.Sprenger[1], M. Weiler[2], and D. Tetzlaff[1,3,4]

[1]Northern Rivers Institute, University of Aberdeen, Aberdeen, UK, AB24 3UF.

[2]Chair of Hydrology, University of Freiburg, Germany

[3]IGB Leibniz Institute of Freshwater Ecology and Inland Fisheries, Germany

[4]Department of Geography, Humboldt University Berlin, Germany

Abstract

Over a four-month summer period, we monitored how forest (Pinus sylvestris) and heather moorland (Calluna spp. and Erica spp.) vegetation canopies altered the volume and isotopic composition of net precipitation (NP) in a southern boreal landscape in northern Scotland. During that summer period, interception (I) losses were relatively high, and higher under forests compared to moorland (46% of gross rainfall (GR) compared with 35%, respectively). Throughfall (TF) volumes exhibited marked spatial variability in forests, depending upon local canopy density, but were more evenly distributed under heather moorland. In the forest stands, stemflow (StF) was a relatively small canopy flow path accounting for only 0.9-1.6% of NP and only substantial in larger events. Overall, the isotopic composition of NP was not markedly affected by canopy interactions; temporal variation of stable water isotopes in TF closely corresponded to that of GR with differences of TF-GR being -0.52 ‰ for δ^2H and -0.14 ‰ for $\delta^{18}O$ for forests and 0.29 ‰ for δ^2H and -0.04 ‰ for $\delta^{18}O$ for heather moorland. These differences were close to, or within, analytical precision of isotope determination, though the greater differences under forest were statistically significant. Evidence for evaporative fractionation was generally restricted to low rainfall volumes in low intensity events, though at times subtle effects of liquid-vapour moisture exchange and/or selective transmission though canopies were evident. Fractionation and other effects were more evident in StF but only marked in smaller events. The study confirmed earlier work that increased forest cover in the Scottish Highlands will likely cause an increase in interception and green water fluxes at the expenses of blue water fluxes to streams. However, the low energy, humid environment means that isotopic changes during such interactions will only have a minor overall effect on the isotopic composition of NP.

Key words: Forest hydrology, interception, throughfall, isotopes, canopy, boreal forest

1. Introduction

Vegetation canopies play a critical role in partitioning gross precipitation (GR) into interception (I) losses and net precipitation (NP), and the latter's further sub-division into throughfall (TF) and stemflow (StF) (Calder, 2005). The relative importance of these fluxes can vary dramatically between different ecosystems and in contrasting hydroclimatic regions (Bosch and Hewlett, 1982; Levia et al., 2011). Changes in canopy water partitioning potentially have major implications for determining the distribution of NP and the resulting flow paths, storage and mixing of water in the subsurface (Keim et al., 2005; Stockinger et al., 2015). This can also exert a strong influence on catchment scale outputs of water in terms of other "green water" fluxes of transpiration and soil evaporative losses and "blue water" fluxes of drainage to streams (Tetzlaff et al., 2013). Recent work has highlighted that the role of vegetation in such partitioning has been under-researched compared to other hydrological processes. Increased awareness that land management can play a critical role in addressing various water security issues has provided an impetus for more extensive research in plant-water interactions (Calder, 2005; Allen et al, 2017). In addition, climate change is predicted to have far-reaching implications for the ecohydrology of many regions, in terms of changing precipitation regimes and temperatures in ways that may affect canopy routing and plant water availability (Kundzewicz et al., 2007; Rennermalm et al., 2010; Capell et al., 2013). Vegetation communities are highly responsive to such changes by adjusting species composition and distribution, as well as biological productivity (Wookey et al., 2009). For example, in many high latitude northern ecosystems, vegetation changes driven by recent climatic warming have been reported, with an expansion of shrub and tree cover accompanying climatic amelioration (Menard et al., 2013; Tetzlaff et al., 2014). The implication of such changes for water partitioning as well as for "blue" and "green" water fluxes and other water balance components at the catchment scale is usually unknown and is still a major research challenge (Bring et al., 2016).

Previous plot scale work has provided a basis for assessing the influence that vegetation canopies can have on precipitation inputs. The fraction of precipitation intercepted by forest and shrub canopies and which is evaporated or sublimated directly back to the atmosphere has been measured in numerous studies (Levia et al., 2011). Similarly, the relative importance of TF, which encompasses canopy drip and water falling through canopy gaps, and StF draining down tree stems has been quantified at many experimental sites (Levia et al., 2011; Allen et al., 2014). Together, TF and StF usually account for about 70-90% of the GR in forested ecosystems, with the remaining 10-30% being lost to I; exact effects vary with hydroclimate and forest type and I losses can be as large as 50% (Levia and Frost, 2003; Allen et al., 2017). However, the resulting heterogeneity and spatial variability of TF and StF can affect soil wetting patterns, soil water re-distribution and groundwater recharge in ways that are still poorly understood (Ford and Deans, 1978; Keim et al, 2006; Guswa and Spence, 2012).

As well as determining the physical quantity of NP, the partitioning of water in vegetation canopies also affects the physical and chemical characteristics of evaporated I and the residual NP (e.g. Soulsby and

Reynolds, 1994; Bhat et al., 2011). For example, stable isotopes of water, deuterium (^{2}H) and oxygen 18 (^{18}O), are commonly used as assumed conservative environmental tracers to identify sources and track the movement of water in catchments (Allen et al., 2017; Makoto et al., 2000; Soulsby et al., 2015). Variation in isotope signatures can be caused by fractionation occurring with the phase changes of water in the canopy, as well as exchange between liquid and vapour water and selection of different canopy flow paths in contrasting events (Yurtsever and Gat, 1981; Rozanski et al., 1993; Ingraham, 1998; Gat et al., 2001; Gat and Tzur, 1968; Allen et al., 2015). It has become apparent that changes to the isotopic composition of water routing through vegetation canopies can have significant effects on the resulting isotopic characteristics of TF and StF at a range of spatial and temporal scales (e.g. Cappa et al., 2003; Liu et al., 2008). For example, Brodersen et al. (2000) showed that the $\delta^{18}O$ compositions of TF and GR were significantly different through isotopic fractionation in the canopy generating enriched TF (Saxena, 1986; Dewalle and Swistock, 1994). Exchange with water vapour and time variant mixing along different canopy flow paths in different precipitation can also alter the isotopic composition of TF and StF, with the effects usually being most marked in StF which often has a longer contact time with vegetation surfaces (Saxena 1986; Brodersen et al., 2000). Liu et al., (2008) also concluded that the isotopic composition of TF can be altered by canopy structure and ongoing evaporation processes. They found a high correlation between canopy structure and evaporation during low intensity rainfall events. However, other experiments in several forest stands failed to find any relationship between the enrichment of isotopes in TF and I rates (e.g. Allen et al., 2014; Hsuch et al., 2006).

It is clear that many of the basic mechanisms and drivers of vegetation-influenced isotopic transformations remain poorly understood (Allen et al., 2017). Also, the extent of such processes in different ecosystems with contrasting hydroclimatic regimes is largely unknown (Tetzlaff et al., 2015). This is an important research gap as the isotopic composition of GR is often used in catchment travel time assessments (Stockinger et al., 2015) or tracer-aided runoff models (Soulsby et al., 2015). If canopy fractionation and other transformative processes are significant, and the isotopic composition of NP is significantly different to GR, then the results of such modelling may be biased and misleading (e.g. Sprenger et al., 2016; Sprenger et al., 2017)

Here, we present results from a study in a headwater catchment in a wet, low energy environment in the Scottish Highlands where we investigated the effects of contrasting dominant vegetation covers on canopy partitioning and the implications for the isotopic composition of NP in TF and StF. In addition to climate-induced changes, forest cover is increasing in many parts of Scotland as a result of the restoration of de-forested moorlands as part of conservation schemes and demands for increased biofuel production (Scottish Forest Strategy, 2006). A move to increased forest cover has the potential to significantly increase I losses, reduce NP and affect the spatial and temporal distribution of soil moisture, groundwater recharge and runoff generation, as well as their associated isotopic composition (Haria and Price, 2000, Tetzlaff et al., 2013, Capell et al., 2013). Our specific objectives were to (i) quantify the influence of canopy cover of contrasting vegetation types on I losses and the partitioning of TF and StF; (ii) characterise the temporal dynamics of I and precipitation partitioning; and (iii) assess the associated influence of vegetation on spatio-temporal dynamics in isotopic composition of TF and StF in a low energy environment.

2. Study Site

The study was conducted in the Bruntland Burn (Figure 1), a 3.2 km² tributary of the larger Girnock catchment (31km^2) and a long-term monitoring site for Atlantic salmon in the Cairngorms National Park in NE Scotland (Soulsby et al., 2016). The climate is maritime at the temperate/boreal transition with mean annual temperatures of around 6.8 °C, with January and July daily averages of 1.2 °C and 12.4 °C, respectively. The mean annual precipitation (P) is about 1000 mm. Most P falls in low intensity frontal events, with ~50 % and ~75 % falling in events of < 10 mm and < 20 mm, respectively (Tetzlaff et al., 2014). Mean annual potential evapotranspiration (PE) and runoff are about 400 mm and 700 mm, respectively. Most evaporation is focused in the relatively short summer period between May and August (Wang et al., 2017). In general, the catchment has limited influence of snow (<5% of the annual GR). The highest P is most likely to occur between November and February, but large events can happen throughout the year. The catchment's elevation ranges between 248 and 539 m with an average of 350 m. Mean slopes are 13° (Birkel et al., 2011; Tetzlaff et al., 2014). The area has been repeatedly glaciated and following the last glacial period, altitudes below 400 m are characterised by drift-draped topography, with poorly sorted till deposits being dominant (Soulsby et al., 2016). Freely draining podzols are the main soils and are found on the steeper slopes covering around 60% of the catchment (Birkel et al., 2011; Tetzlaff et al., 2014; Dick et al., 2015), mainly facilitating groundwater recharge.

The most extensive vegetation is heather (Calluna vulgaris and Erica tetralix) moorland over the podzol soils. The heather is around 0.3m high, with an extensive (up to 80%) canopy coverage. Also on the podzols, there are some stands of native Scots pine (Pinus sylvestris) and birch (Betula pendula) that, due to historic land management, only remain in small areas of the catchment on inaccessible slopes or behind fenced enclosures (Birkel et al., 2011; Tetzlaff et al., 2014). Past land management resulted in tree clearance in many headwater catchments in the UK. This was carried out to create more productive environments for rearing sheep (Ovis aries), red deer (Cervus elaphus) or red grouse (Lagopus lagopus scotica); the latter two for hunting (Dick et al., 2015). As a consequence, the forest coverage for the entire catchment is <15%.

3. Data and Methods

Field sampling was conducted over a four-month summer period between 1st of June until 24th of September 2015. This encompassed the main summer months in the Scottish Highlands when evaporation is highest. The plots were close (<750m) to an automatic weather station (Figure 1) that recorded standard variables at 5 minute intervals (Wang et al., 2017). Four study plots were installed on south and north facing slopes with two sites for each aspect. On each slope, one plot was in the heather shrub vegetation (predominantly Calluna spp. and Erica tetralix spp.) and one in a Scots Pine plantation (Figure 1). In general, the trees were older (ca 50 years), taller (ca 15m) and of greater trunk diameter at the south-facing forest (SF), with this site being more homogeneous overall compared to the north-facing forest (NF) (Table 1). At the NF site, tree characteristics varied from very young (ca 20 years old), small (<5m tall) Scots Pines to a few older trees (ca 50 years) with higher canopy coverage and larger diameter at breast-height (DBH). Median canopy coverage, estimated from digital photography (see below) ranged from 67% on the NF to 69% on the SF, though there was marked variability at each site for individual TF collectors. For the heather, the vegetation canopy was more regular and typically 0.2-0.3m high, though gaps appeared between plants or where the canopy of older plants had a more open structure. Median canopy coverage (from the digital photography ranged between 62% for the south-facing heather (SH) site and 65% for the north-facing heather (NH) site (Table 1). The heather sites were in stands where Calluna vulgaris is the dominant species, with a canopy height of around 0.3m.

The sites were equipped with a total of 75 TF and 10 StF collectors. The TF collectors comprised a lower base that was secured to the ground and an inner cylinder with a measuring scale on it which collected water from an open funnel with a 78.5 cm^2 orifice. To prevent leaves and litter plugging the entry of the collector, a plastic mesh was fixed to the base of the funnel. The TF collectors were randomly located in 20 x 20 m grids for each site. These grids were sub-divided into 25 4 x 4 m sub-grids, giving a stratified random sample to capture variability in canopy cover. 25 TF collectors in each of the forest sites were used to account for the greater spatial variability compared to the more uniform heather sites, which had 10 collectors at each site. The percentage canopy cover at each collector determined by digital photography varied between 0% and 81%, though the median values for each site were similar (ranging between 62-69%, Table 1). For further comparison, one open collector was also located next to each plot and at the weather station in the valley bottom, to capture potential differences in the amount of GR. There was no significant difference between the GR sampled by these collectors and the weather station rain gauge station (one-way ANOVA, p=0.59) so GR sums and maximum intensity over each sampling period could be calculated. All TF and StF samples were protected with a small aliquot of paraffin shown in previous tests to prevent fractionation. As part of longer-term monitoring in the Girnock, daily precipitation samples were also collected for isotope analysis and could be used to complement the coarser sampling of TF and StF in this study (Soulsby et al, 2015).

For the StF measurements and sampling, 10 trees of different height, DBH and species (Birch and Scots Pine) were selected; 5 in each forest plot. The DBH of all the trees in a grid was measured to estimate the tree basal area (BA) in the grid. Following Reynolds and Stevens (1987), a 30-40 cm section at approximately 1.50 m height above the ground and free of whorls and branches was cleaned of loose debris and moss, whilst avoiding damage to the tree's bark. A PVC flexible tube with a diameter of 15 mm was wrapped around this area in a single spiral to cover the circumference of the tree. The tube was adjusted using four to five plastic pipe clips. The gap between the tree's bark and the tubing was sealed with silicon and a silicon "lip" at the edge of the tube was created to form a gutter to collect StF. Small holes cut into the tube every 10-20 cm allowed the StF to drain to a plastic container with a capacity of

15 l. Again, paraffin was added to prevent fractionation. Given time and resource constraints, it was considered impractical to assess StF down individual heather plants, thus, we recognised our measurement of NP by TF would be a conservative under-estimate.

Intervals between sample collection ranged from 4 to 14 days (depending on logistical constraints and the occurrence of precipitation events), generating a data set of 16 sampling occasions. For each of the 75 TF collectors, the amount of TF was determined and an isotope sample was taken. Isotope samples were transferred into 8 ml glass vials with a silicone seal to prevent evaporation. The StF in the 10 collectors was measured (if present) and sampled on the same dates as the TF. To determine the amount for each plot, the volume of water in each collector was measured and normalised by dividing by the tree basal area, with the average for 5 trees being scaled up for the total basal area. An isotope sample was taken for StF.

Samples were stored in a fridge until analysis. Samples were filtered and 1 ml was injected into 1.5 ml glass vials in accordance with the procedures detailed in Los Gatos Research Inc. (2010). The samples were analysed for the stable isotopes of water δ^2H and δ^{18}O using an off-axis integrated cavity laser spectrometer (a Los Gatos DLT-100 Liquid Water Isotope Analyser). In the post analysis, the sample ratios of δ^{18}O and δ^2H were derived by calibration against known standards relative to the Vienna Standard Mean Ocean Water (VSMOW, Green et al., 2015). The precision of the isotope analysis is reported by the manufacturer to be +/-0.1 ‰ for δ^{18}O and +/-0.4 ‰ for δ^2H and this corresponded to our own assessments.

I loss and NP were calculated for all sites. For the forest sites, I loss was calculated using the following equation (Helvey and Patric, 1965: Crockford and Richardson, 2000):

$$I = GR - TF - StF \qquad \text{(Eqn 1)}$$

Where I is interception loss [mm]; GR is gross precipitation [mm]; TF is throughfall [mm] and StF is stemflow [mm]. NP is the sum of TF and StF, therefore, I equals GR minus NP (Crockford and Richardson, 2000). For the heather sites, as StF was ignored estimates of I were likely overestimates.

Potential evapotranspiration was calculated using the Penman-Monteith approach, which requires air temperature, radiation, air humidity and wind speed that were recorded at 5 minute intervals at the meteorological station (Figure 1).

For isotopes, the local meteoric water line (LMWL) was determined using a least-squares regression on all GR isotope values sampled during the field season (Dansgaard, 1964; Landwehr and Coplen, 2006):

$$\delta^{2}H = 7.6275 * \delta^{18}O + 2.0779 \qquad \text{Eqn 3}$$

In addition, we also calculated the line conditioned excess (lc-excess [‰]) to describe the offset of a sample from the LMWL, and thus, an indicator of possible non-equilibrium fractionation. It is defined as (Landwehr and Coplen, 2006):

$$lc\text{-excess} = \delta^{2}H - a * \delta^{18}O - b \qquad \text{Eqn 4}$$

Where $\delta^{2}H$ and $\delta^{18}O$ are the $\delta^{2}H$/ $\delta^{18}O$ values of the samples [‰] and a and b are the slope and intercept of the LMWL which then (combined with Eqn 3) gives Eqn 5 to calculate the lc-excess for the TF, StF and open test collectors at all sites:

[illegible] = δ[illegible] $-$ 7.6275 * [illegible] $-$ 2.0779 Eqn 5

The precision of the isotopes analysis resulted in a precision of the lc-excess of +/-1.16 ‰. To derive one (weighted and representative) lc-excess value of TF, StF and open test collectors at each sample date, volume weighted δ^2H and $\delta^{18}O$ values were used to calculate the lc-excess for each site. δ^2H and $\delta^{18}O$ were weighted using the TF/StF volume of the related collector. It should be noted, however, that the use of the LMWL in the lc-excess calculations still means that the deviations for individual events may not be captured as specific event water lines may differ.

A general characterization of the study site was undertaken using the program ArcGIS version 10.3.1 (Figure 1). A slope map of the catchment was produced using a high resolution Digital Elevation Model. Canopy coverage [%] - defined as the fraction of soil that is covered by the vegetation's canopy - was calculated for the whole catchment as well as for the two forest grids using airborne Light Detection and Ranging (LiDAR) 1*1m data. In addition, digital photography and the free software CAN-EYE V6.1 developed at the EMMAH laboratory (Mediterranean Environment and Agro-Hydro System Modelisation) were used to calculate the canopy coverage for each collector individually (CAN-EYE user manual). Using hemispherical images, it was necessary to integrate the cover fraction over a range of zenith angles as it was impossible to maintain exact nadir direction. This range as well as the lens properties can then be changed prior to analysing the photos. Light contamination due to direct sunlight was corrected in the program.

Correlations between variables were described by Pearson correlation (r) for normally distributed data and with the Spearman rank correlation (ρ) if the Shapiro-Wilk test for normality revealed that the data was not drawn from a normal distribution. Wilcoxon signed rank tests were used to test for differences between data sets (with $p < 0.05$ for significance).

4. Results

4.1 Variability in hydroclimate

Hydroclimatic conditions were highly variable during the summer of 2015, which was cooler than average, with periods of day time maximum temperatures substantially >20°C restricted to a few days in early June and late June/early July (Figure 2). Mean daily air temperatures varied between 7.0 and 15.4 °C with marked diurnal ranges (Figure 2b). Mean relative humidity was 77.2% with lowest values during daytime during the warm early summer periods, and highest in mid and end of August and September (Figure 2c). Mean wind speeds were moderate (2.7 m s^{-1}) with higher peaks of 7.5 to 8 m s^{-1} during some sampling periods (Figure 2d). Precipitation totalled 270 mm for the four-month period; the highest daily total was 26.2 mm on 17th July and intensities reached up to 4 mm h^{-1} in the same July period. Around 30% of the precipitation fell in low intensity events below 5 mm d^{-1} and around 60% on days with < 10 mm d^{-1} (Figure 2e). During most of the individual sampling periods (i.e. the time between emptying the collectors) a sum of GR between 5 mm and 20 mm was typically recorded. The highest measured sum of GR was 74.8 mm over a 14 days sampling period in July. The lowest measured sum of GR was 0.8 mm over a 7-day period in September. Total potential evapotranspiration (PET) was 216 mm for the whole sampling period of 4 months (with a daily mean of 2.2 mm).

4.2 Variability in interception, throughfall and stemflow

The dominant pathways of GR at all sites was either TF or I evaporated back to the atmosphere (Table 2). I losses were generally highest in the two forest plots (46% average) compared with the two heather plots (34% average) (Figure 3). A Wilcoxon signed rank test showed that TF was always less than GR and inter-site differences between the two vegetation types were significant ($p < 0.05$) on seven of the sampling dates, with TF in Scots pine being lower on all but one of the sampling dates (9th June) (Figure 3a). Regarding temporal variability, TF exhibited a strong positive and exponential correlation with GR at each site for each sampling period, with the relationship slightly stronger for the forest sites. Conversely, percentage I losses were negatively correlated with GR amount, with percentage loss much higher in smaller events (Table 2, Figure 4a). Similar, though generally weaker negative relationships were evident between I and maximum rainfall intensity in the sample period (Figure 4b). When the maximum GR intensity was about 1.5 mm h^{-1}, the I loss was usually lowered to <70% of GR. Correlation with other climatic factors showed much weaker or insignificant relationships.

To understand intra-site differences within the forest plots, Figure 5 shows the mean weighted amount of TF. At both sites, highest TF tended to be measured in the collectors located in canopy gaps and with greater distance to the trees. Conversely, the TF amount was low in areas with very dense canopy cover and in close proximity to a tree's stem, especially at the NF (Figure 5a). Distance to the closest tree stem was correlated with TF amount (p-values for NF ≤0.001; SF ≤ 0.05); on average TF increased by 8.8% per metre from each tree. The I loss was significantly correlated with canopy cover for both sites ($\rho = 0.80$ for NF, $\rho = 0.62$ for SF). Lower intra-site variability could be found at the SF site (Figure 5b) as there, trees were more evenly spread over the grid with less variability in canopy cover and tree size distribution. At the SF site, the weighted mean amount in TF as a fraction of GR per collector over all sample dates was 58.2 % with a minimum and maximum of 17.7 % and 75.4 % for individual collectors, respectively. The mean TF of all collectors – as a fraction of the sum of GR – was 51.8 % for the NF site with a minimum of 8.4 % for the collectors under the densest canopy and a maximum of 79.6 % for a collector where the canopy had a more open structure.

StF was a small fraction of GR at the forest sites accounting for 1.6 % and 1.0% of incoming precipitation for the NF and SF, respectively. StF amounts were highly variable over the sampling periods and were most strongly correlated with GR ($r = 0.76$, $p<0.001$) at both sites. There were three sampling occasions for the NF and four for the SF where no StF was generated.

For the heather plots, TF accounted for 60% and 67% of incoming precipitation at the NH and SH sites, respectively. Again, total GR input exhibited the strongest correlation with TF amount in each sampling period (Figure 4). Intra-site variability of TF amount was marked, though usually less than for the forests (cf generally more restricted ranges in Figure 3). There was a negative relationship between canopy cover and the amount of TF for both sites, though this was only significant ($\rho = -0.74$, $p = 0.01$) for the NH site.

4.3 Vegetation influences on the isotopic composition of net precipitation

The isotopic composition of precipitation was temporally variable with δ^2H ranging between -115.0‰ to -14.0‰ in GR and $\delta^{18}O$ between -15.2‰ and 0.9‰ (Figure 6 and Table 3). Isotopic signatures were most depleted during the first sampling periods (early June) when mean air temperature were lowest (~7°C), reflecting the influence of rainfall brought on by northerly air streams. Thereafter, prevailing winds had a stronger south westerly component bringing rainfall more enriched with heavier isotopes as is typical for summer.

The isotopic composition of GR and TF under both land covers were strongly correlated (for δ^2H and δ^{18}O, r was >0.85 and >0.90 for all sites, respectively ($p<0.001$)). Air temperature was also positively correlated with both isotopes in GR (r = 0.76, $p<0.001$) and TF under both land use types (r = 0.58, p=0.03 for heather, r = 0.59, p = 0.02 for forest). Volume weighted isotopic compositions in TF samples at all sites were similar to the weighted isotopic composition of GR, though overall TF under the forests was slightly more depleted than for moorland (Table 4). The overall differences of TF-GR being -0.52 ‰ for δ^2H and -0.14 ‰ for δ^{18}O for forests and 0.29 ‰ for δ^2H and -0.04 ‰ for δ^{18}O for heather moorland. These small differences between the land cover types were significant ($p<0.05$) on 10 sampling occasions, and significant differences to GR were far more common under forests (Figure 6).

To assess any offset of the TF and StF isotopic signature from the LMWL, lc-excess was calculated as an indicator of evaporative fractionation (Figure 6b). Gross precipitation/rainfall lc-excess values were close to zero for much of the study period, with more negative values (indicative of fractionation and moisture recycling) in early June, early July and mid-August. LC-excess in TF also varied throughout the study period but mostly followed the lc-excess patterns of in rainfall (GR/open collectors) for both land cover types. Significant differences ($p<0.05$) between land cover types only occurred on four occasions whist the lc-excess for forest sites was significantly different to that of GR on four occasions, heather – GR differences were only evident once.

The isotope values of all the TF and StF samples (>1100) for each sampling period were plotted in dual isotope space to explore the potential effects of evaporative fractionation and other processes in modifying the composition of NP beneath the two vegetation canopies (Figure 7). The majority of TF samples from the forest and heather moorland sites mostly scattered along the LMWL and occupied overlapping space, with the forest samples usually, but not always, being more variable. Despite the overall, longer-term small differences in the composition of TF compared to GR, there could be surprising variation between individual collectors for specific sampling events. The position of samples for both land covers relative to the LMWL line, and degree of offset, varied over the course of the season. For example some dates showed clear evidence of evaporative fractionation (e.g. 9th June, 2nd July and 6th and 13th August). Other dates, like 6th July and 24th September had a large number of samples plotting above the LMWL. This, together with the variable scatter on individual sampling dates, indicates potential subtle effects of event-based variability in the MWL, event-specific canopy pathways and the possibility of canopy moisture exchange between air and plants. However, in general, the isotopic variability at the two plots, indexed by the standard deviation of δ^2H (same for $\delta^{18}O$– not shown) was negatively correlated with maximum rainfall intensity (more than rainfall amount), with this relationship strongest in the forest (Figure 8). The coefficient of variation (not shown) also showed a similar relationship with rainfall amount and rainfall intensity.

The StF samples likewise generally plotted along the LMWL, but were usually more enriched than GR and TF (Figure 7). The isotopic composition in StF in forest plots was also variable over time, mostly reflecting the variability of the precipitation input signature (Figure 9) with r = 0.92 for δ^2H and r = 0.96 for $\delta^{18}O$). A notable deviation was on 6th July when samples from several collectors plotted above the LMWL, and then again on 30th July where StF was lighter in several samples. Again, these deviations might be explained by vapour-liquid moisture exchange effects, such as condensation on the canopy, or activation of selective canopy flow paths delivering water at specific stages of events where the intra-event isotope changes in rainfall may have occurred.

Notwithstanding such subtle sample-specific differences, overall the spatial variability in the isotopic signatures of TF was limited at all sites. Further, in the forest sites, despite the spatial variation in TF volumes, the isotopic variability between samplers was not marked (Figure 10). There was no distinct pattern of more depleted, i.e. more negative δ^2H values (larger circles) vs. the enriched values (smaller circles) and much of the intra-site variability was small. There was no statistically significant correlation with canopy cover or distance from tree at either site. The heather sites showed similar limited variability.

5. Discussion

5.1 Differences in interception and throughfall between forest and shrub cover

Interception losses for all sites were quite high; averaging up to 35% for heather and 46% for Scots Pine. But these lie within previously reported ranges for pine trees and heather (Calder, 1990; Haria and Prices, 2000; Llorens and Domingo, 2007). For example, for another Scottish site in a wetter area in the western Cairngorms, Haria and Price (2000) found that I losses under Scots Pine were 37% of precipitation but only 13% for heather. This suggests that we may be significantly over-estimating heather losses by not accounting for stem flow. It should also be stressed that as our study was carried out over the summer, the overall annual percentage I losses are likely to be smaller due to the lower atmospheric moisture demand and higher precipitation in winter. In comparison with studies elsewhere, I losses for a Scots pine forest were found to lie between 13% and 49% (Llorens et al., 1997) and similar coniferous trees with comparable interception capacity and branch architecture found respective values ranging from 40 to 41% at a 130 to 170 year old spruce stand in the Black Forest in Germany (Brodersen et al., 2000) with similar figures for a mixed spruce forest in the Eifel national park in Germany (Stockinger et al., 2015). For canopy partitioning in other boreal forests, Ilvesniemi et al. (2010) working on Scots pine in Finland found that the proportion of TF was ~67% of annual precipitation, ~33% was lost as I and, like in our study, StF was small (<1%). However, in dense plantations, Cape et al (1991) showed StF could be as high as 15% in the UK, but TF still dominated accounting for 51-78% of annual precipitation.

The main reason for the high summer I losses at the study site under both forest and heather is probably that much of the precipitation in this part of northern Scotland falls in small, frequent, low intensity events which can interact with the high canopy interception storage (~1-3mm) for both vegetation types (Haria and Price, 2000). Lowest percentage I losses were found in weeks with higher GR amounts and intensities. During weeks with lowest intensity events and low GR totals, I losses were as high as 95% - 100%, whereas for weeks with intensities > 7 mm h^{-1}, losses ranged between 22% - 45% of GR. Scatena (1990) also observed that high forest I losses were attributable to rain events with very low intensities (≤ 2mm h^{-1}) and small storm totals, as such events are similar to canopy storage volumes allowing evaporation to occur. In our study, wind speeds ranged from 2 - 8 m s^{-1}; these moderate to fresh winds (Smyth et al., 2013) help facilitate evaporation from the canopy by turbulent transfer, especially at the forest sites where the canopy is well-ventilated (Herwitz and Slye, 1995).

5.2 Intra-site variation in throughfall

TF fractions were higher for the heather sites compared to the forests, though the intra-site spatial variability was greatest in the forest plots. Lowest TF fractions could be found at the younger NF (Table 2). Canopy coverages for the collectors, derived from digital photography, showed that these contrasts could be partly explained by differences in canopy cover at both forest sites. The NF site was characteristic of a young Scots Pine stand, with high canopy density, particularly in the middle part of the plot. Usually, mature Scots pine is characterized by a low density and open canopy (Hall et al., 2001) like at the SF site. Tree sizes, age, crown density and canopy coverage of the collectors varied at the NF site as shown in Figure 5 whereas all of those attributes were fairly uniform for the SF (reflected in the low standard deviation of canopy cover; Table 1). Statistically significant correlations could be found between I values for the two forest sites and both canopy coverage and distance to the closest tree. Similar relationships have been shown by previous studies (e.g. Stout and MacMahon, 1961; Helvey and Patric, 1965; Aussenac 1970; Johnson, 1990). The effect was most marked during small precipitation events, when the rainfall intensity is similar to the canopy interception capacity; as the TF amount and variability is greatest as GR will be intercepted by the canopy and most NP will reach the ground through canopy gaps. As the GR increases and the canopy storage gets increasingly saturated, each additional increment of rainfall generates TF reducing spatial variability (Loustau et al., 1992). Influences of the canopy coverage and distance to the nearest tree stem on TF were more marked for the NF, as vegetation cover is more heterogeneous there. For the two heather sites, TF was more evenly distributed and lacked a consistent relationship with canopy cover.

Our study also showed that a GR threshold of approximately 15 mm was needed for all of the TF collectors in the forest sites to collect a sample. This partly reflects the high interception capacity above some collectors in the forest plots with high canopy coverage. Marin et al. (2000) also found high variabilities due to a suite of interacting controlling factors, particularly the local canopy density and architecture, which regulates the redistribution of incident precipitation and associated flow paths. Despite this, as shown by other studies (e.g. Marin et al., 2000; Peng et al. 2014; Stockinger et al., 2015), a strong positive correlation between TF volume and the total amount of GR could be found at all sample sites and collectors. However, other studies for Scots Pine have shown contrasting conditions. For example, Kowalaska et al (2016) found that for Scots pine, the amount of TF water did not show a significant relationship with LAI, canopy cover or the distance to the nearest tree trunk. Rather the canopy partitioning of water was strongly modified by the irregular structure of the crowns and the irregular distribution of the trees in the stand as well as by weather conditions.

5.3 The role of stem flow

As noted above, StF comprised a relatively small proportion of the NP at the two forest sites. To generate StF, canopy and bark water storage have to be filled and rainfall amounts have to be sufficient to wet the tree stem enough for continuous flow to reach the ground (Allen et al., 2017). Different GR amounts and intensities have been shown to trigger StF for different trees (> 7mm for beech and >10 mm for Scots pine); independent of species, the threshold above which StF generation did not increase with higher amount of GR was ~25 mm. Mean and median StF were mainly dependent on maximum rainfall. Xiao et al. (2000) and André et al. (2008) found that higher wind speeds increased the StF production as they reduced the initiation threshold by blowing canopy stored water onto the tree trunk; however, no direct correlation was found here. Similarly, no correlation between DBH and StF amount was evident. A more detailed investigation of the vegetation cover (such as crown area, branch architecture, bark composition) would be needed to improve the prediction of StF generation. However, previous studies (e.g. Ford and Deans, 1978; Loustau et al., 1992) have shown that the interactions of vegetation-related controls on StF and hydroclimatic drivers are difficult to disentangle to explain StF amounts and variations between individual trees. Despite its minor overall importance, in larger events StF can still provide a large localised flux of water into the soil and its role in influencing spatial variations in soil moisture and groundwater recharge are poorly understood.

5.4 Influence of vegetation cover on spatio-temporal dynamics in isotopic compositions

Temporal variability in the isotopic TF signature was found to be mostly driven by the variability in the incoming GR isotopic composition. In contrast to the strong influence of canopy cover on the volume and re-distribution of NP, the overall associated effects on the isotopic composition of TF and StF were small, though some subtle effects were detected for individual sample events. At all four sites, the average composition of TF little changed compared to GR, though the overall effects were greater under the forests. Other studies have found much stronger influences of canopy cover on the isotopic signature of NP (e.g. Ikawa et al., 2011; Stockinger et al., 2015). There was no statistical relationship between TF isotopic composition and GR amount or maximum intensity. Similar low correlations have also been observed by Allen et al. (2015) for a Douglas-fir dominated catchment in northern Oregon and Kato et al. (2013) for a cypress plantation in eastern Japan. However, the variability of the TF isotopic signal tends to be higher for lower GR amounts and intensities (Figure 8).

The lc-excess of GR and TF exhibited highly correlated temporal variability at all sites, fluctuating between close to zero and more negative values. For some samples in each month, the effect of moisture recycling and evaporative fractionation on GR isotopic composition may have been evident in the observed negative lc-excess values during this period. Alteration of the GR isotopic composition by its passage through the canopy can result from evaporative losses, mixing processes along selective flow paths and isotopic exchange with atmospheric water vapour (Saxena, 1986; Tsujimura and Tanaka, 1998). These exchange processes can potentially lead to both depletion and enrichment in isotopic signatures depending on ambient conditions. Such effects were small overall, though they were evident during specific sample periods.

Compared to the temporal variability in TF isotopic composition, spatial variability between and within the forest and heather moorland sites was found to be small, similar to other studies (Brodersen et al., 2000). The TF isotopic variability in the forests was found to be slightly higher compared to the heather sites, which are characterised by a more uniform canopy cover. Differences in isotopic composition within a site could be marked at the scale of individual sampling periods. Likely explanations probably relate to event-scale conditions such as the changing isotopic composition of rainfall relative to the spatial and temporal variation of activation of flow paths through the canopy, and moisture exchange with the atmosphere (e.g. evaporative fractionation and condensation) (Brodersen et al., 2000; Kato et al., 2013; Allen et al., 2014). However, more intense sampling during and after events would be needed to test such hypotheses. For example, Kato et al. (2013) also found that in tree canopies there may be a forest edge effect, where TF nearer the edge - where the canopy is more ventilated - might be changed isotopically as a result of higher evaporative losses. In contrast, collectors below less dense canopies might gather more direct TF and can therefore show a similar isotopic composition to precipitation (Kato et al., 2013).

StF isotopic compositions were more markedly different to those compared to TF in the two forest sites. This probably reflects the longer contact time of StF and greater opportunities for fractionation or moisture exchange with the atmosphere (Ikawa et al., 2011). StF is also more likely affected by activation of flow paths later in events with mixing processes and bark storage delaying StF initiation depending on prevailing meteorological conditions (e.g. rainfall intensity, wind speed etc.) (Levia and Herwitz, 2005; Staelens et al., 2008; Ikawa et al., 2011). However, event-based sampling would be needed to further explore this.

Our study demonstrated the importance of vegetation characteristics such as canopy coverage, age, height, density, DBH on TF amounts in a northern landscape, but less influence on isotopic composition. Given the limited changes in the isotopic composition of NP below the forest and heather canopies, it is reasonable to use GR isotope values in travel time estimates and tracer-aided runoff models in this geographical region, though correcting for canopy effects is possible. There is little evidence to suggest that this will cause a significant additional source of uncertainty to such models, but there may be some more unusual events where correction could help. More broadly, better understanding of rainfall partitioning processes through canopy cover is important, especially in relation to likely future vegetation changes driven by a changing climate (Tetzlaff et al., 2013). Many northern landscapes are already experiencing and responding to those shifts (Tetzlaff et al., 2014). Climate projections for Scotland predict longer dry and warm periods and shifting precipitation patterns (Capell et al., 2013). This, combined with large scale afforestation plans by the Scottish government (The Scottish Forestry Strategy, 2006) will be likely to affect vegetation distribution and community as well as linked flow path partitioning and water balances. This leads to an increasing importance in understanding vegetation influences on water partitioning, storage dynamics and water availability in higher latitude catchments (Geris et al., 2015).

6. Conclusions

We analysed TF and StF with respect to their spatial and temporal variability in quantity and isotopic composition under forest (Scots Pine) and shrub (heather) cover during a four-month summer period in a northern landscape. We identified large temporal differences in TF which were mainly governed by the size of rainfall events and intensity. Interception was highest under forest cover (46%) where TF exhibited marked spatial variability in relation to canopy density and structure. I losses under heather were probably <35%, with TF more uniformly distributed. The contribution of StF to the overall water balance was found to be relatively small (~ 1% of GR). StF was found to correlate most strongly with maximum precipitation intensity. The subsequent I losses were in the upper range of reported literature values for coniferous forest stands. This probably reflects both the local hydroclimate where most rainfall events are frequent and small (<5mm) with low intensity, and high wind speeds are common. Vegetation canopies had a less marked effect on the isotopic composition of NP. Overall, the isotopic composition of NP was not markedly affected by canopy interactions; temporal variation of stable water isotopes in TF closely tracked that of GR with differences of TF-GR being -0.52 ‰ for δ^2H and -0.14 ‰ for δ^{18}O for forests and 0.29 ‰ for δ^2H and -0.04 ‰ for δ^{18}O. These differences were close to, or within, analytical precision of isotope determination, though they were statistically significant. Evidence for evaporative fractionation was generally restricted to low rainfall volumes in low intensity events, though at times subtle effects of liquid-vapour moisture exchange and/or selective transmission though canopies were evident. Further event-scale work is needed to elucidate these processes.

Acknowledgements

We thank the European Research Council ERC (project GA 335910 VEWA) for funding the VeWa project and The Leverhulme Trust (project PLATO, RPG-2014-016) for funding.

REFERENCES

Allen, S. T., Brooks, J. R., Keim, R. F., Bond, B. J., McDonnell, J. J., 2014. The role of pre-event canopy storage in throughfall and stem flow by using isotopic tracers. Ecohydrology, 868(July 2013), 858–868. http://doi.org/10.1002/eco.1408.

Allen, S.T., Keim, R. F., McDonnell, J. J., 2015. Spatial patterns of throughfall isotopic composition at the event and seasonal timescales. Journal of Hydrology, 522, 58–66. http://doi.org/10.1016/j.jhydrol.2014.12.029.

Allen ST, Keim RF, Barnard HR, McDonnell JJ, Brooks JR. (2017) The role of stable isotopes in understanding rainfall interception processes: a review. WIREs Water 2017, 4:e1187. doi: 10.1002/wat2.1187

André F., Jonard M., Ponette Q., 2008. Influence of species and rain event characteristics on stemflow volume in a temperate mixed oak-beech stand. Hydrol. Process 22:4455–4466.

Aussenac, G., 1970. Action du couvert forestier sur la distribution au sol des prècipitations. Annales des Sciences Forestières 27, 383–399.

Bhat, S. Jacobs, J.M. and Bryant, M.L. 2011. The Chemical Composition of Rainfall and Throughfall in Five Forest Communities: A Case Study in Fort Benning, Georgia Water Air Soil Pollut (2011) 218:323–332

Birkel, C., Tetzlaff, D., Dunn, S. M., Soulsby C., 2011. Using lumped conceptual rainfall-runoff models to simulate daily isotope variability with fractionation in a nested mesoscale catchment, Adv. Water Resour., 34(3), 383–394.

Bosch, J. M. and Hewlett, J. D., 1982. A review of catchment experiments to determine the effect of vegetation changes on water yield and evapotranspiration, J. Hydrol., 55, 3–23.

Bring, A., I. Fedorova, Y. Dibike, L. Hinzman, J. Mård, S. H. Mernild, T. Prowse, O. Semenova, S. L. Stuefer, and M.-K. Woo (2016), Arctic terrestrial hydrology: A synthesis of processes, regional effects, and research challenges, J. Geophys. Res. Biogeosci., 121, 621–649, doi:10.1002/2015JG003131

Brodersen, C., Pohl, S., Lindenlaub, M., Leibundgut, C., Wilpert, K., 2000. Influence of vegetation structure on isotope content of throughfall and soil water. Hydrol. Processes 14, 1439–1448.

Calder, I.R. 1990 Evaporation in the uplands, Wiley and Sons Chichester.

Calder, I. R. (2005), Blue Revolution: Integrated Land and Water Resource Management, pp. 353, Earthscan, London.

CAN-EYE user manual, Weiss, M., Baret, F., 2014. CAN-EYE V6.313 USER MANUAL. EMMAH, INRA, Science & Impact, 76p.

Capell, R., Tetzlaff, D., & Soulsby, C., 2013. Will catchment characteristics moderate the projected effects of climate change on flow regimes in the Scottish Highlands? Hydrological Processes, 699(December 2012), 687–699. http://doi.org/10.1002/hyp.9626.

Cappa, C. D., Hendricks, M. B., DePaolo, D. J., Cohen R. C., 2003. Isotopic fractionation of water during evaporation, J. Geophys. Res., 108(D16), 4525, doi: 101029/2003JD003597.

Crockford, R. H., Richardson, D. P., 2000. Partitioning of rainfall into throughfall, stemflow and interception: effect of forest type, ground cover and climate. Hydrological Processes, 2920(April 1999), 2903–2920.

Dansgaard, W. (1964), Stable isotopes in precipitation, Tellus, 16(4), 436–468, doi:10.1111/j.2153-3490.1964.tb00181.x.

Dewalle D.R., Swistock B.R., 1994. Differences in Oxygen-18 content of throughfall and rainfall in hardwood and coniferous forests. Hydrological Processes 8:75–82. DOI: 10.1029/94WR00758.

Dick, J.J., Tetzlaff, D., Birkel, C., Soulsby, C., 2015. Modelling landscape controls on dissolved organic carbon sources and fluxes to streams. Biogeochemistry, vol 122, no. 2-3, pp. 361-374.

Ford, E.D., Deans, J.D., 1978. The effect of canopy structure on stemflow, throughfall and interception loss in a young Sitka spruce plantation. J. Appl. Ecol. 15, 905– 917.

Gat, J.R., Mook, W.G., Meijer, A.J., 2001. Atmospheric water. Environmental isotopes in the hydrological cycle -Principles and applications, Vol. 2. W.G. Mook (Ed.) IHP-V, Technical Document N. 39, UNESCO, Paris. 113p.

Gat, J.R., Tzur, Y., 1968. Modification of the isotopic composition of rainwater by processes which occurs before groundwater recharge. In: Isotope Hydrology, Proc. Symp. Vienna 1966, International Atomic Energy Agency, pp. 49–60.

Geris, J., Tetzlaff, D., McDonnnell, J., & Soulsby, C., 2015. The Relative Role of Soil Type and Tree Cover on Water Strorage and Transmission in Northern Headwater Chatchments. Hydrological Processes.

Green M.B., Laursen B.K., Campbell J.L., McGuire K.J., Kelsey E.P., 2015. Stable water isotopes suggest sub-canopy water recycling in a northern forested catchment. Hydrological Processes. DOI: 10.1002/hyp.10706.

Guswa A, Spence C., 2012. Effect of throughfall variability on recharge: application to hemlock and deciduous forests in western Massachusetts. Ecohydrology 5: 563–574.

Hall, J.E., Kirby, K.J., Whitbread, A.M., revised 2004. National vegetation classification field guide to woodland, 117 pages A5 softback, ISBN 1 86107 554 5.

Haria A. and Price D. 2000; Hydrology and Earth System Science, Evaporation from Scots pine (Pinus sylvestris) following natural re-colonisation of the Cairngorm mountains, Scotland. 4, 451-461, Helvey, J., & Patric, J. H., 1965. Canopy and Litter Interception of Rainfall by Hardwoods of Eastern United States. Water Resources Research, 1(2), 193–206.

Herwitz S.R., Slye R.E., 1995. Three-dimensional modeling of canopy tree interception of wind-driven rainfall. J Hydrol. 168:205–226.

Hsueh, Y. H., Allen, S. T., & Keim, R. F. (2016). Fine-scale spatial variability of throughfall amount and isotopic composition under a hardwood forest canopy. Hydrological Processes.

Ikawa, R., Yamamoto, T., Shimada, J., & Shimizu, T., 2011. Temporal variations of isotopic compositions in gross rainfall, throughfall, and stemflow under a Japanese cedar forest during a typhoon event. Hydrological Research Letters, 5, 32–36. http://doi.org/10.3178/HRL.5.32

Ingraham, N.L., 1998. Isotopic variations in precipitation. Isotope Tracers in Catchment Hydrology (C.Kendall, C., J.F. McDonnel, Eds) Elsevier, Amsterdam, Chapter 3, .87–118.

Johnson, R.C., 1990. The interception, throughfall and stemflow in a forest in highland Scotland and the comparison with other upland forests in the UK. J. Hydrol. 118, 281–287

Kato, H., Onda, Y., Nanko, K., Gomi, T., & Yamanaka, T., 2013. Effect of canopy interception on spatial variability and isotopic composition of throughfall in Japanese cypress plantations. Journal of Hydrology, 504, 1–11. http://doi.org/10.1016/j.jhydrol.2013.09.028

Keim, R. F., Skaugset, A. E., & Weiler, M. (2005). Temporal persistence of spatial patterns in throughfall. J. Hydrol., 314(1), 263–274

Keim, R. F., Tromp-van Meerveld, H. J., and McDonnell, J. J. (2006) A virtual experiment on the effects of evaporation and intensity smoothing by canopy interception on subsurface stormflow generation, J. Hydrol., 327, 352–364.

Kundzewicz, Z. W., Mata, L. J., Arnell, N., Döll, P., Kabat, P., Jiménez, B., Miller, K., Oki, T., Şen, Z. & Shiklomanov,I., 2007. Freshwater resources and their management. Climate Change 2007: Impacts, Adaptation and Vulnerability. Contribution of Working Group II to the Fourth Assessment Report of the Intergovernmental Panel on Climate Change (ed. by M. L. Parry, O. F. Canziani, J. P. Palutikof, P. J. van der Linden & C. E. Hanson), 173–210. Cambridge University.

Landwehr, J.M. and Coplen, T.B., 2006. Line-conditioned excess: a new method for characterizing stable hydrogen and oxygen isotope ratios in hydrologic systems, in Isotopes in Environmental Studies, Aquatic Forum 2004: International Atomic Energy Agency, Vienna, Austria, IAEA-CSP-26, p. 132–135.

Levia, D.F., Frost, E.E., 2003. A review and evaluation of stemflow literature in the hydrologic and biogeochemical cycles of forested and agricultural ecosystems. Journal of Hydrology 274 (1–4), 1–29.

Levia DF, Herwitz SR. 2005. Interspecific variation of bark water storage capacity of three deciduous tree species in relation to stemflow yield and solute flux to forest soil. Catena; 64:117–37.

Levia, D. F., Keim, R. F., Carlyle-Moses, D. E., Frost, E. E., 2011. Throughfall and Stemflow in Wooded Ecosystems (pp. 425–443). http://doi.org/10.1007/978-94-007-1363-5

Liu, W.J., Liu, W.Y., Li, J.T., Wu, Z.W., Li, H.M., 2008. Isotope variation of throughfall, stemflow and soil water in a tropical rain forest and a rubber plantation in Xishuangbanna, SW China. Hydrol. Res. 39, 5–6.

Llorens P., Domingo F., 2007. Rainfall partitioning under Mediterranean conditions. A review of studies in Europe. J Hydrol 335:37–54.

Llorens P., Poch R., Latron J., 1997. Rainfall interception by a Pinus sylvestris forest patch overgrown in a Mediterranean mountainous abandoned area I. monitoring design and results down to the event scale. J Hydrol 199:331–345.

Los Gatos Research Inc, 2010. Liquid Water Isotope Analyser. User Manual. Los Gatos Research, Inc. 67 East Evelyn Avenue, Suite 3, Mountain View, CA 94041-1529

Loustau, D., Berbigier, P., Granier, A., Hadj Moussa, F. E., 1992. Interception loss, throughfall and stemflow in a maritime pine stand. I. Variability of throughfall and stemflow beneath the pine canopy. Journal of Hydrology, 138, 449–467.

Makoto T, Tomoe N, Norio T, Jun S., 2000. Stable isotope studies of precipitation and river water in the Lake Biwa basin, Japan. Hydrological Processes 14: 539–556.

Marin, C.T., Bouten, W., Sevink, J., 2000. Gross rainfall and its partitioning into throughfall, stemflow and evaporation of intercepted water in four forest ecosystems in western Amazonia. J. Hydrol. 237, 40–57. http://dx.doi.org/ 10.1016/S0022-1694(00)00301-2.

Menard, C. B., R. Essery, and J. Pomeroy (2014), Modelled sensitivity of the snow regime to topography, shrub fraction and shrub height, 315, Hydrol. Earth Syst. Sci., 18, 2375–2392.

Molina, A. J., del Campo, A. D., 2012. Forest Ecology and Management "The effects of experimental thinning on throughfall and stemflow: A contribution towards hydrology-oriented silviculture in Aleppo pine plantations. Forest Ecology and Management, 269, 206–213. http://doi.org/10.1016/j.foreco.2011.12.037.

Peng, H. H., Zhao, C. Y., Feng, Z. D., Xu, Z. L., Wang, C., Zhao, Y., 2014. Canopy interception by a spruce forest in the upper reach of Heihe River basin, Northwestern China, Hydrol. Processes, 28(4), 1734–1741.

Rennermalm, A.K., Wood, E.F., Troy, T.J., 2010. Observed changes in pan-arctic cold season minimum monthly river discharge. Climate Dynamixy 35(6): 923-939.DOI.10.1088/1748-9326/4/2/024011.

Reynolds, B., Stevens, P. A., 1987. British Geomorphological Research Group Technical Bulletin no. 36, 42-55. Geobooks, Norwich.

Rozanski, K., Araguás-Araguás, L., Gonfiantini, R., 1993. Isotopic Patterns in Modern Global precipitation. Climate Change in Continental Isotopic Records (P.K. Swart, K.L. Lohmann, J.

McKenzie, S. Savin, Eds) Geophysical Monograph 78, American Geophysical Union, Washington, DC, 1–37.

Saxena R.K., 1986. Estimation of canopy reservoir capacity and Oxygen-18 fractionation in throughfall in a pine forest.NordicHydrology 17:251–260.

Scatena, F. N., 1990. Watershed scale rainfall interception on two forested watersheds in the Luquillo mountains of Puerto Rico, Journal of Hydrology, 113, pp.89–102.

Sprenger, M, Tetzlaff D, Soulsby C. Stable isotopes reveal evaporation dynamics at the soil–plant–atmosphere interface of the critical zone. Hydrology and Earth System Sciences (HESS-D), in review.

Sprenger, M., Leistert, H., Gimbel, K., & Weiler, M. (2016). Illuminating hydrological processes at the soil-vegetation-atmosphere interface with water stable isotopes. Reviews of Geophysics, 54(3), 674–704.

Soulsby, C. and Reynolds, B. (1994) The chemistry of throughfall, stemflow and soil water beneath broadleaved woodland and moorland vegetation in upland Wales. Chemistry and Ecology, 9, 115–134.

Soulsby, C., Birkel, C., Geris, J., Dick, J., Tunaley, C. & Tetzlaff, D. 2015. Stream water age distributions controlled by storage dynamics and nonlinear hydrologic connectivity: Modeling with high–resolution isotope data. Water Resources Research, vol 51, no. 9, pp. 7759–7776.

Soulsby, C. Birkel, C. and Tetzlaff, D. (2016) Characterising the age distribution of catchment evaporative losses. Hydrological Processes. DOI:10.1002/hyp.10751.

Staelens, J., Schrijver, A.D., Verheyen, K., Verhoest, N.E.C., 2006. Spatial variability and temporal stability of throughfall water under a dominant beech (Fagus sylvatica L.) tree in relationship to canopy cover. J. Hydrol. 330, 651–662.

Staelens, J., Schrijver, A.D., Verheyen, K., Verhoest, N.E.C., 2008. Rainfall partitioning into throughfall, stemflow, and interception within a single breech (Fagus sylyatica L.) canopy: influence of foliation, rain event characteristics, and meteorology. Hydrological Processes 22(1): 33–45. doi:10.1002/hyp.6610.

Stockinger, M. P., Lücke, A., McDonnell, J. J., Diekkrüger, B., Vereecken, H., & Bogena, H. R., 2015. Interception effects on stable isotope driven streamwater transit time estimates. Geophysical Research Letters, 42(1), 5299–5308. http://doi.org/10.1002/2015GL064622.

Stout, B. B., McMahon, R. J., 1961. Throughfall variation under tree crowns, J. Geophys. Res., 66, 1839–1843.

Tetzlaff D., Soulsby C., Buttle J., Capell R., Carey S.K., Kruitbos L., Laudon H., McDonnell J., McGuire K., Seibert S., Shanley J., 2013. Catchments on the Cusp? Structural and functional change in northern ecohydrological systems. Hydrological Processes 27: 766–774.

Tetzlaff, D., Birkel, C., Dick, J.J., Geris, J. & Soulsby, C., 2014. Storage dynamics in hydropedological units control hillslope connectivity, runoff generation, and the evolution of catchment transit time distributions. *Water Resources Research*, vol 50, no. 2, pp. 969–985.

Tetzlaff, D., Buttle, J., Carey, S. K., Mcguire, K., Laudon, H., Soulsby, C., 2015. Tracer‐based assessment of fl ow paths, storage and runoff generation in northern catchments – a review. Hydrol. Processes, 3490 (December 2014), 3475–3490. http://doi.org/10.1002/hyp.10412

The Scottish Forestry Strategy, 2006. Forestry Commission Scotland, Edinburgh.

Tsujimura, M., Tanaka, T., 1998. Evaluation of evaporation rate from forested soil surface using stable isotope composition of soil water in a headwater basin. Hydrol. Processes 12, 2093–2103.

Wang H, Tetzlaff D, Dick J, Soulsby C. (2017) Assessing the environmental controls on Scots pine transpiration and the implications for water partitioning in a boreal headwater catchment. *Agricultural and Forest Meteorology*, 10.1016/j.agrformet.2017.04.002.

Wookey, P.A., Aerts, R., Bardgett, R.D., Baptist, F., Brathen, K.A., Cornelissen, J.H.C., Gough, L., Hartley, I.P., Hopkins, D.W., Lavorel, S., Shaver, G.R., 2009. Ecosystem feedbacks and cascade processes: understanding their role in the responses of arctic and alpine ecosystems to environmental change. Global Change Biology 15: 1153–1172.

Xiao, Q., McPherson, E.G., Ustin, S.L., Grismer, M.E., 2000. A new approach to modeling tree rainfall interception, J. Geophys. Res., 105(D23), 29173–29188, doi:10.1029/2000JD900343 .

Yurtsever, Y., Gat, J.R., 1981. Atmospheric waters. Stable Isotope Hydrology: Deuterium and Oxygen‐18 in the Water Cycle. (J.R. Gat, R. Gonfiantini, Eds) Technical Reports Series 210, IAEA, Vienna, 103–142.

Tables:

Table 1: Vegetation characteristics of the 4 sampling plots: Number of trees at the forests sites, Mean diameter at breast height (DBH), median distance to collector and canopy coverage for each of the four sites. The values derived using digital photography represent only the collector's canopy coverage whereas the values calculated using the LiDAR data are mean values for the whole site.

				Canopy coverage based on					
				Digital photography (CAN-EYE)					LiDAR Data (ArcGIS)
Site	# of trees	Mean tree DBH [cm]	Median distance of trees to collector [m]	Min [%]	Max [%]	Median [%]	Mean [%]	Std Dev [%]	Mean [%]
NF Northfacing forest	36	13.8	1	28	81	67	63	16.3	43
NH Northfacing Heather	0	-	-	0	79	65	60	21.8	-
SF Southfacing Forest	46	21.8	1.5	50	74	69	68	5.8	68
SH Southfacing Heather	0	-	-	0	78	62	53	24.3	-

Table 2 Sampling dates, the number of their integrating days, gross rainfall, maximum rainfall intensity, arithmetic mean throughfall amount and sample number for forest and heather site, stemflow volumes in forest.

		Gross rainfall		Forest		Heather		Forest	
Sampling day	sampling integrated days	precipitation sum [mm]	maximum intensity [mm h^{-1}]	n	TF [mm]	n	TF [mm]	n	StF [mm]
2015-06-01	11	7.6	3.8	50	2.5±2.2	22			
2015-06-09	8	12.2	0.8	50	6.1±1.9	22	3.2±3.4	10	0.39±0.46
2015-06-17	8	3.6	0.4	50	0.8±0.8	22	1.2±0.8	10	0
2015-06-25	8	10.4	1.8	49	4.3±2.9	22	6.3±2.6	10	0.08±0.01
2015-07-02	7	10.4	4.6	49	3.0±2.5	22	5.6±1.9	10	0.04±0.07
2015-07-06	4	20.8	4.6	49	15.6±4.2	22	15.6±6.1	10	1.22±0.85
2015-07-20	14	74.8	7.6	50	48.9±13.9	22	52.4±19.0	10	3.15±1.91
2015-07-30	10	23.6	8	50	13.2±5.7	22	15.0±4.2	10	3.68±2.26
2015-08-06	7	12.8	1.6	50	4.1±2.7	22	7.1±2.3	10	0.12±0.12
2015-08-13	7	2.2	1.2	50	0.2±0.3	22	0.5±0.2	10	0
2015-08-19	6	36.2	3.8	50	21.3±7.3	22	22.1±6.5	10	1.71±1.34
2015-08-28	9	18.8	1.8	49	9.6±4.6	22	11.8±4.3	10	0.49±0.39
2015-09-03	6	8.8	3	49	3.0±1.9	22	4.0±1.6	10	0.08±8
2015-09-10	7	0.8	0.2	50	0.0±0.1	22	0.0±0.1	10	0
2015-09-18	8	16.8	3.2	50	8.9±3.4	22	10.5±3.5	10	0.57±37
2015-09-24	6	16	4.6	50	10.7±3.4	22	11.6±3.6	10	0.88±46
Mean values		17.2 ± 17.7	3.2 ± 2.3	9.5 ± 12 (55 % of GR)		11.1 ± 13 (64 % of GR)		0.82 ± 1.2 (1.3 % of GR)	

Table 3 Overview of stable isotope data (‰) for the gross rainfall, throughfall in forest, throughfall in heather and stemflow at trees.

	Gross precipitation				Throughfall Forest				Throughfall Heather				Stem flow Forest			
Day	n	δ^2H	$\delta^{18}O$	lc-excess	n	δ^2H	$\delta^{18}O$	lc-excess	n	δ^2H	$\delta^{18}O$	lc-excess	n	δ^2H	$\delta^{18}O$	lc-excess
2015-06-01					42	-95.7±4.7	-12.3±0.7	-4.5±1.4					7	-99.4±11.3	-12.6±1.9	-5.7±3.8
2015-06-09	3	-96.4±6.2	-12.5±1.0	-3.4	36	-96.9±17.1	-12.3±3.0	-4.2±2.2	9	-94.1±5.1	-12.0±0.9	-4.7±1.9		±	±	±
2015-06-17	3	-33.6±6.5	-5.27±0.8	2.4	33	-38.4±8.3	-5.4±0.9	-1.6±2.8	15	-30.1±6.0	-4.7±0.7	1.7±1.4	8	-29.5±7.5	-4.1±0.9	-2.4±3.4
2015-06-25	3	-38.1±1.6	-5.22±0.2	-2.5	45	-37.7±7.2	-5.3±0.7	-1.7±2.6	21	-39.4±4.7	-5.4±0.5	-2.5±2.1	3	-24.8±11.7	-2.2±1.8	-12.8±3.2
2015-07-02	3	-24.7±0.8	-3.05±0.1	-6.2	40	-28.7±4.1	-3.6±0.6	-5.7±2.7	22	-25.4±2.2	-3.2±0.5	-5.4±3.3	10	-39.2±1.7	-6.0±0.5	2.8±4.1
2015-07-06	3	-40.4±0.4	-5.6±0.1	-1.9	50	-40.3±1.7	-5.8±0.3	-0.3±1.6	22	-41.2±1.7	-6.0±0.3	0.8±1.7	10	-57.3±5.3	-8.4±1.0	3.6±2.8
2015-07-20	3	-58.5±0.4	-8.15±0.1	0.2	50	-57.1±1.3	-8.3±0.2	2.4±1.8	22	-59.2±4.2	-8.5±0.8	1.9±2.8	7	-52.5±5.3	-7.5±0.9	1.4±2.3
2015-07-30	3	-46.9±0.4	-6.52±0.1	-1.1	46	-48.3±2.4	-6.7±0.4	-0.9±3.3	22	-47.1±1.6	-6.4±0.2	-2.0±1.5	10	-15.2±2.4	-2.0±0.5	-4.8±3.1
2015-08-06	3	-25.3±0.5	-3.71±0.1	-1.6	42	-21.3±3.2	-3.4±0.5	0.0±2.9	22	-25.2±2.6	-3.5±0.6	-3.4±4.2		±	±	±
2015-08-13	3	-47.8±0.6	-5.27±0.9	-11.8	23	-43.6±5.5	-5.5±0.8	-5.9±4.1	20	-47.0±5.8	-5.8±0.7	-6.6±4.2	10	-60.6±4.1	-8.3±0.5	-0.4±0.7
2015-08-19	3	-64.7±0.4	-8.92±0.1	0.0	50	-59.0±3.6	-8.1±0.5	-0.8±1.9	22	-63.3±2.0	-8.7±0.3	-0.4±1.4	10	-30.5±4.0	-4.3±0.5	-2.1±3.1
2015-08-28	3	-42.2±0.6	-6.19±0.1	1.1	49	-36.8±4.6	-5.5±0.6	1.0±2.9	21	-40.1±3.1	-6.0±0.3	1.8±1.8	8	-50.0±4.3	-6.6±0.5	-3.5±1.06
2015-09-03	1	-53.5	-7.1	-2.9	47	-56.4±3.3	-7.4±0.4	-3.5±0.9	21	-54.9±2.9	-7.3±0.3	-3.0±1.0		±	±	±
2015-09-18	3	-55.1±0.7	-8.1±0.0	3.3	50	-53.6±5.6	-7.8±0.7	2.2±3.3	22	-56.7±2.6	-8.1±0.3	1.9±2.2	10	-43.0±3.2	-6.6±0.3	3.1±1.8
2015-09-24	3	-52.8±0.8	-7.3±0.2	-0.8	50	-51.5±1.6	-7.4±0.5	1.0±4.5	22	-52.6±1.3	-7.4±0.4	0.1±3.1	10	-49.4±1.2	-7.0±0.2	0.3±1.0
Mean values		-48.6±18.5	-6.6±2.4	-1.8±3.8		-47.8±18.0	-6.6±2.2	-1.2±2.7		-48.3±17.9	-6.6±2.3	-1.4±2.9		-41.1±14.5	-5.7±2.3	-1.2±4.5

Figures

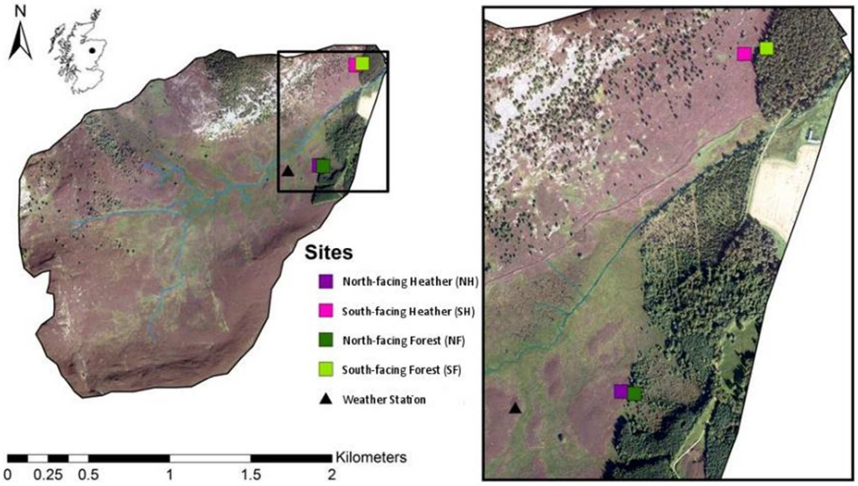

Figure 1: Bruntland Burn catchment with all the site locations and the Bruntland Burn stream. Locations of collectors are pictured in differently coloured squares.

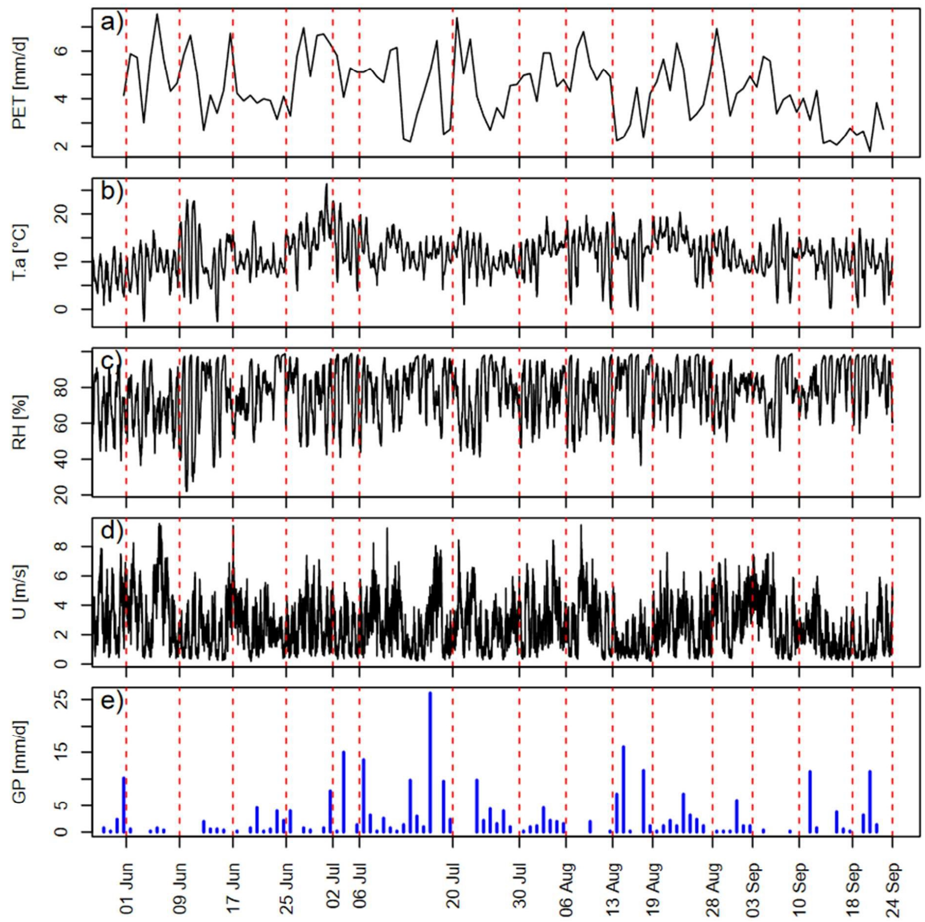

Figure 2: Hydroclimatic conditions: (a) Daily potential Evapotranspiration (PET [mm/ d] (Pennman-Monteith), (b) Air temperature (T.a [°C], (c) humidity (RH [%]), (d) wind speed (U [m s^{-1}]) and (e) daily precipitation (GR [mm d^{-1}]) during the study period. The vertical orange lines represent the sampling dates. Apart from GR and PET (daily), hourly values are shown.

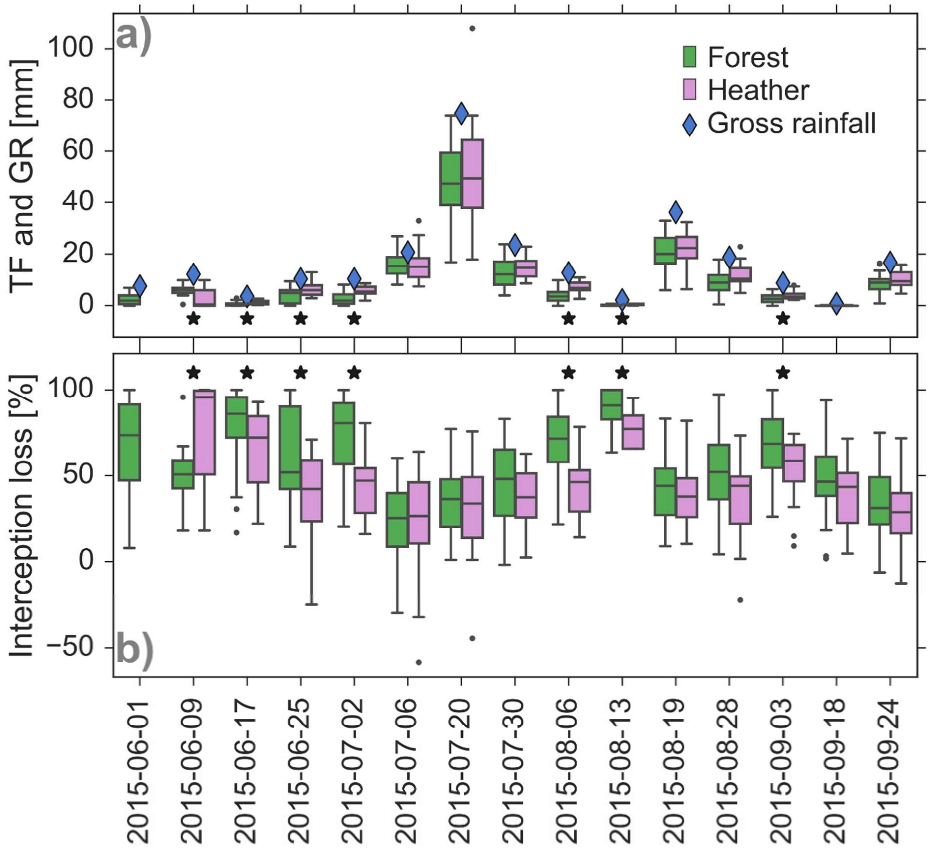

Figure 3: a) Throughfall TF in forest and heather (green and purple boxplots, respectively) and gross rainfall GR (blue diamond) amount. GR was always significantly higher than TF. b) Boxplots showing TF fraction in % (TF as fraction of GR) for forest and heather sites. Outliers are marked as points. For both subplots, asterisks indicate significant differences ($p<0.05$) between forest and heather (Wilcoxon test).

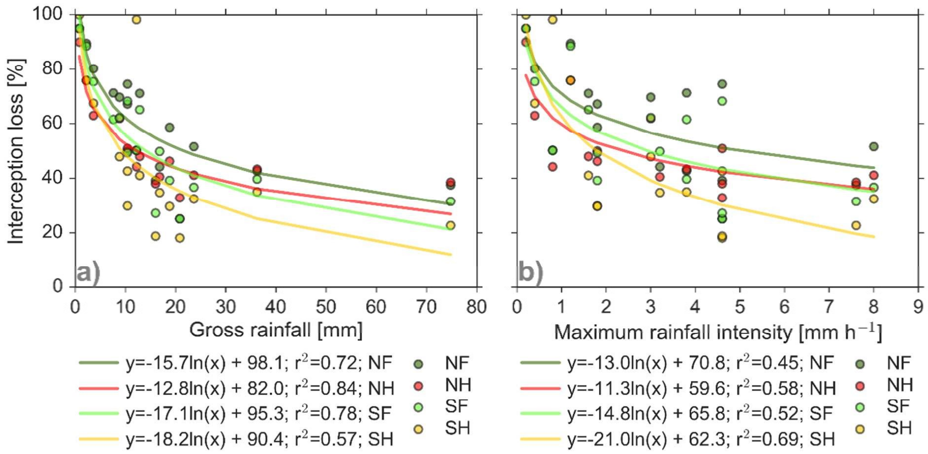

Figure 4 a) Relationship between the interception loss and the gross rainfall amount and b) maximum rainfall intensity during each sampling period for the four study sites. The lines show a logarithmic fit to the data points. The equation and the coefficient of determination for the fitted curves are given.

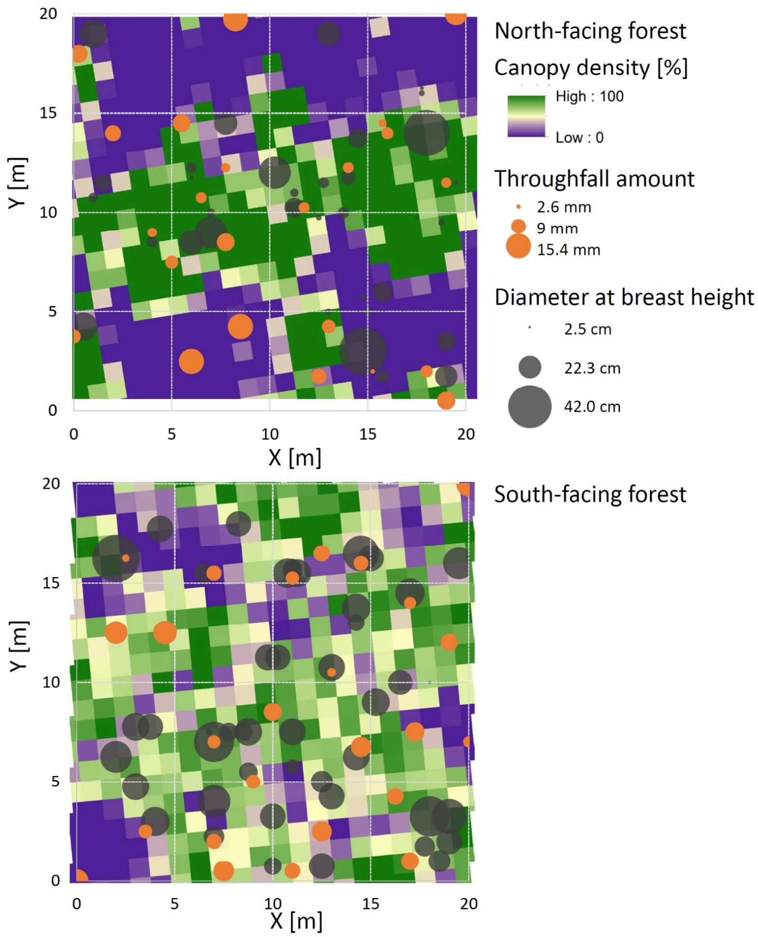

Figure 5: 20 x 20 m grid of both forest sites with TF collectors and trees (black dots). The size of the orange points represents the average TF (over all sample dates) and the size of the black dots represent the DBH. Dark green squares indicate high canopy coverage, purple indicates no canopy coverage [%] as derived from LIDAR measurements.

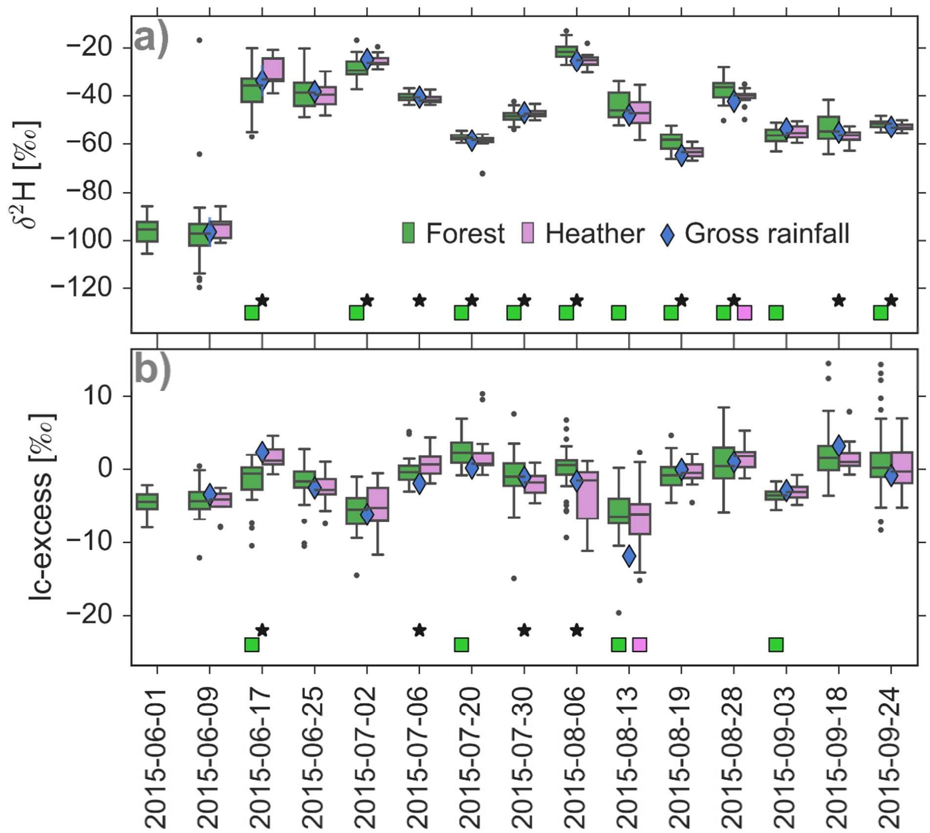

Figure 6: a) δ^2H and b) lc-excess of TF in forest and heather (green and purple boxplots, respectively) and in gross rainfall (blue diamonds) for each sampling campaign. Stars indicate significant differences ($p<0.05$) between forest and heather. Green and purple boxes below boxplots indicate significant differences between TF and GR for forest and heather, respectively. Outliers are marked as points.

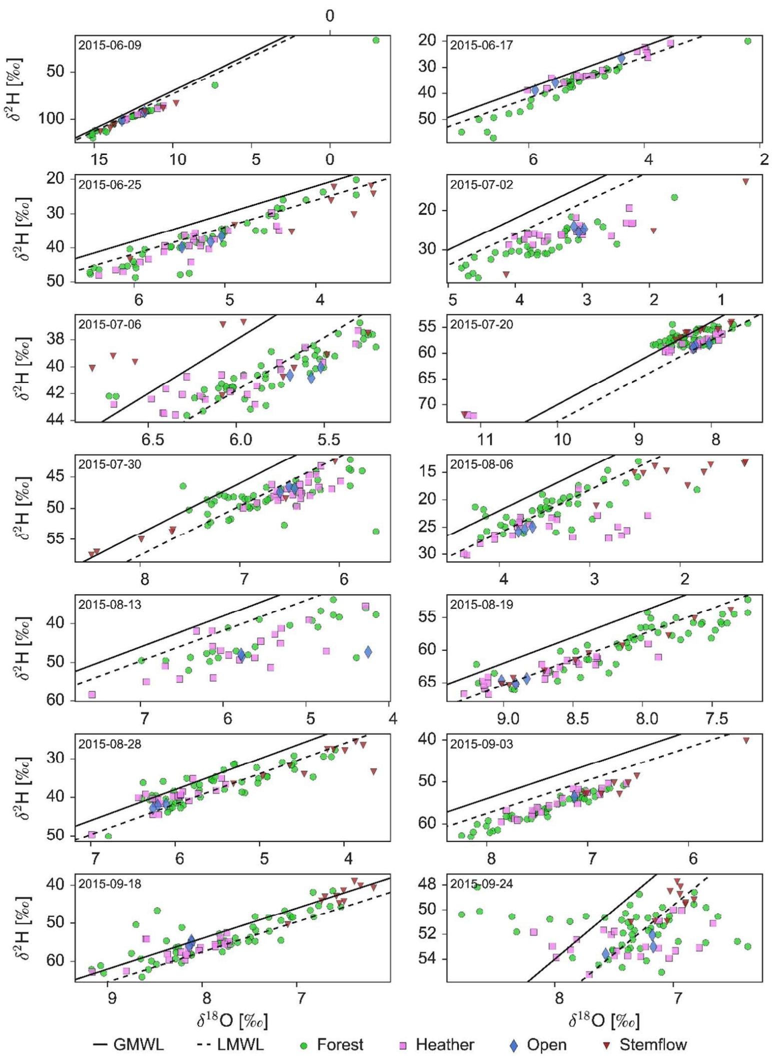

Figure 7: Dual isotope plots of all isotope samples for each sampling date over the entire sampling period. Green circles represent the forest sites, pink squares represent the heather sites. Blue diamonds are open collector of gross rainfall and brown triangles is stemflow. The dashed line shows the Local Meteoric Water Line (LMWL), the continuous line the Global Meteoric Water Line (GMWL).

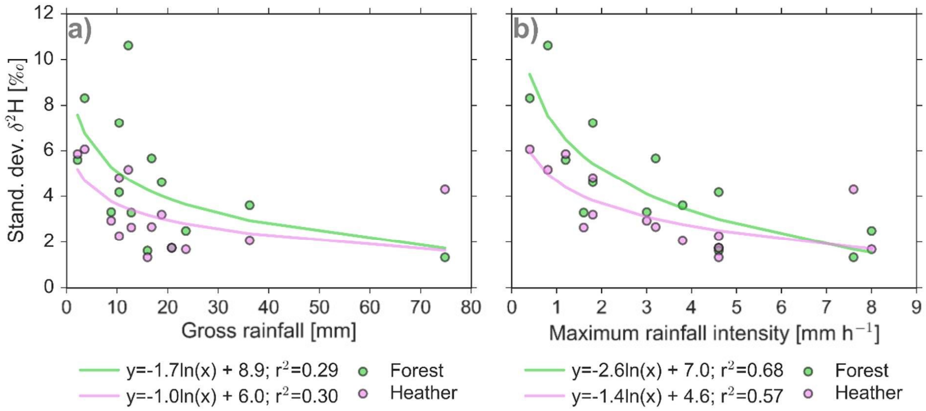

Figure 8: Relationship between standard deviation of the δ^2H values of the throughfall in the forested (green) and heather (purple) sites and the gross rainfall amount (a) and the maximum rainfall intensity (b) during the integrated sampling interval. The lines show a logarithmic fit to the data point s. The equation and the r^2 for the fitted curves are given.

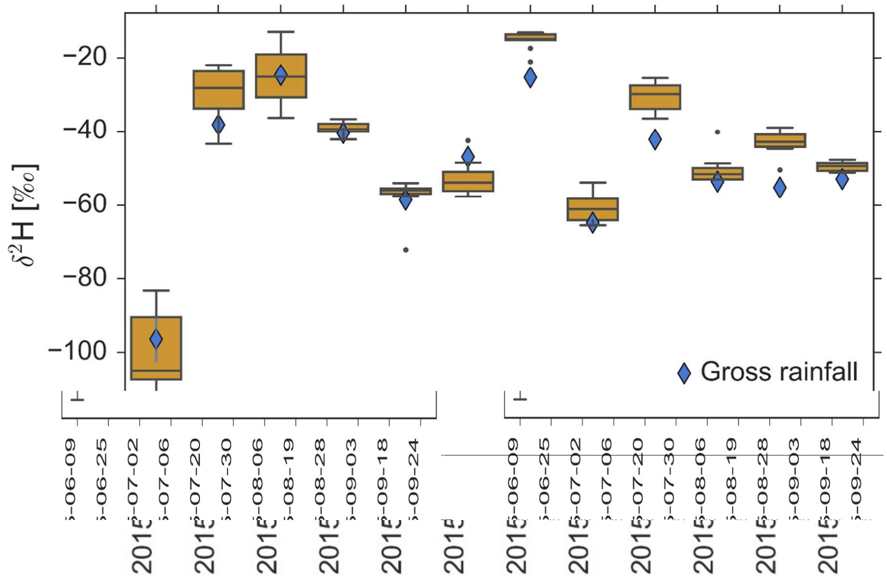

Figure 9: Tree stemflow d^{2}H in comparison with gross rainfall (blue diamonds).

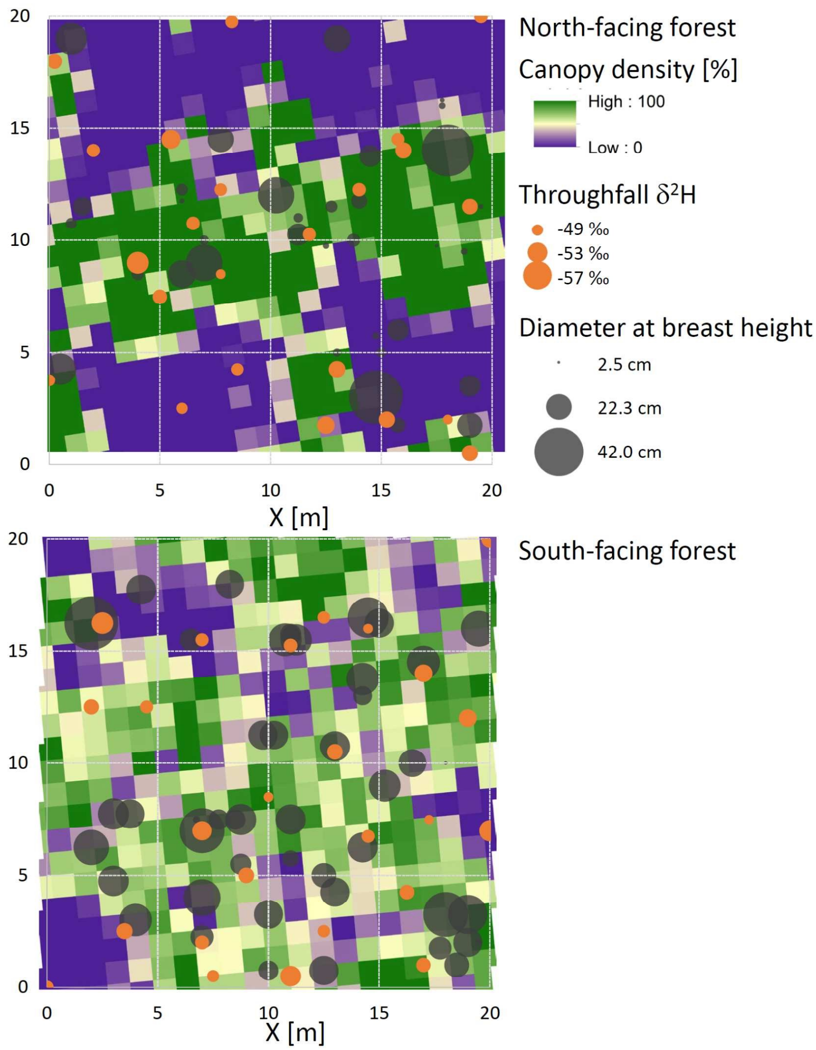

Figure 10: 20x20m grid of both forest sites with TF collectors (orange dots) and trees (black dots). The size of the orange points represent the average δ^2H values and the size of the black dots represent the DBH. Dark green squares indicate high canopy coverage [%], purple indicates no canopy coverage as derived from LIDAR measurements.